

J. P. B. C. de Melo · B. El-Bennich · T. Frederico

The photon-pion transition form factor: incompatible data or incompatible models?

Received: date / Accepted: date

Abstract The elastic and $\gamma \rightarrow \pi$ transition form factors of the pion along with its usual static observables are calculated within a light-front field approach to the constituent quark model. The focus of this exercise in a simple model is on a unified description of all observables with *one* singly parametrized light-front wave function to detect possible discrepancies in experimental data, in particular the contentious large momentum-squared data on the transition factor as reported by BaBar and Belle. We also discuss the relation of a small to vanishing pion charge radius with an almost constant pion distribution amplitude and compare our results with those obtained in a holographic light-front model.

Keywords Light Front Field Theory · Axial Anomaly · Electromagnetic Form Factors · Neutral Pion

1 Plaidoyer for a consistent and uniform analysis

The experimental findings of the BaBar Collaboration [1] on the $\gamma \rightarrow \pi$ transition form factor in the anomaly-driven reaction $\gamma^* \gamma \rightarrow \pi^0$ stirred some attention in the hadron community. Indeed, while the BaBar data is in agreement with earlier experiments on a domain of squared-momentum transfer below $Q^2 = -q^2 \lesssim 10 \text{ GeV}^2$ [2; 3], the data points at larger Q^2 values remarkably exceed the prediction of perturbative QCD (pQCD) in the asymptotic limit [5; 6]. In contrast, a more recent measurement by Belle [4] appears to corroborate the pQCD prediction, although one ought to really appreciate the meaning of “asymptotic”: namely that the asymptotic parton distribution amplitude (PDA) on the light front, $\phi_\pi^{\text{asy}} = 6x(1-x)$, is not an appropriate description of the meson’s internal structure at scales currently available in experiments [7; 8; 9].

On the other hand, at the relevant momentum scale of the $\gamma^* \gamma \rightarrow \pi^0$ transition [1], it was shown [10; 11; 12; 13; 14; 15; 16; 17] that PDA modifications, as advocated by the studies in Refs. [18; 19; 20; 21; 22], lead to form factors which deviate drastically from its QCD asymptotic form. The resulting distributions, $\phi(x) \neq \phi_\pi^{\text{asy}}$, are constant or at least non-vanishing $\forall x \in [0, 1]$ and characterize an essentially point-like pion [10]. One comes to a similar conclusion within the framework of a light-front quark model [16] and the impact of the form of the PDA on numerical results has been discussed in detail in Ref. [13]. These overly flat distributions cannot be reconciled with nonperturbative studies of the pion’s Bethe-Salpeter amplitude [8].

João Pacheco B. C. de Melo (E-mail: joao.mello@cruzeirosul.edu.br)
Laboratório de Física Teórica e Computacional, Universidade Cruzeiro do Sul, 01506-000, São Paulo, Brazil

Bruno El-Bennich
Laboratório de Física Teórica e Computacional, Universidade Cruzeiro do Sul, 01506-000, São Paulo, Brazil.

Tobias Frederico
Instituto Tecnológico de Aeronáutica, 12228-900, São José dos Campos, Brazil.

The process $\gamma^*\gamma \rightarrow \pi^0$ is very interesting in its own right. If one wants to describe the entire domain of experimentally explored momentum transfer within a unique theoretical framework, it must simultaneously account for the nonperturbative Abelian anomaly and the functional behavior of perturbative QCD. Studies based on perturbation theory and model input which solely aim at higher-order precision in PDA calculations cannot catch the full extent of the nonperturbative nature of light hadron bound states. Essential contributions stemming from the dressing of the fermions and gauge bosons are lost and can lead to unnatural predictions, such as a double-dip structure of the pion's PDA, a feature neither congruent with one's intuition about the Goldstone boson nor with nonperturbative continuum studies [9; 23].

In practical calculations of the pion's static properties and form factors, one is thus left with the choice to use the most advanced contemporary nonperturbative QCD tools, for examples lattice-regularized QCD [24; 25] and the combined approach of Dyson-Schwinger and Bethe-Salpeter equations [26; 27], or alternatively use models whose connection to QCD is not straightforward yet with its guidance allow for successful numerical results and predictions. We here discuss such a QCD-based model on the light front [31; 32; 33; 34] and refer the reader to the more recent approach of light-front holography discussed by Stan Brodsky in this meeting [35].

In Ref. [16], we investigated the effect of varying wave functions in a given established light-front quark model for the pion [36; 37; 38] applied to the triangle diagram which describes the $\gamma^*\gamma \rightarrow \pi^0$ transition. The nonperturbative contributions to this reaction are not dynamically generated in this approach but encoded in the parametrized wave functions and constant mass function of the dressed quark propagators. The point of the exercise is not to test the state-of-the-art Bethe-Salpeter amplitude for a given decay or transition, but rather to apply this model to all relevant observables. These are the static properties, the pion decay constant and electric charge radius, and the elastic and transition form factors. The weak decay constant, f_π , serves to adjust the unique parameter that enters the bound-state wave function and introduces a mass scale. This fixed parameter is then used to compute the charge radius and the form factors. No adjustment is made in the process to accommodate a specific observable unless it is made *consistently and uniformly* to all observables, the reason for which is rather simple: should we find a wave function, or implicitly the pion's PDA since $\Phi_\pi \equiv \Phi(\mathbf{k}_\perp, x)$, whose functional behavior leads to the rise of the $\gamma \rightarrow \pi$ transition form factor observed in the BaBar data, the same wave function must yield an elastic form factor as well as a decay constant and charge radius consistent with well known experimental values [39].

As we show in Section 3, the light-front calculations with a given wave function reproduce rather well the weak decay constant, charge radius, elastic form factor and the pion-photon transition form factor *if* these form factors tend toward the asymptotic pQCD limit. It is not possible to reconcile both the BaBar and Belle data above $q^2 \simeq 20 \text{ GeV}^2$ with our model which prefers the Belle results. Nonetheless, we can adapt the parameter and achieve a transition form factor which partially accounts for the rising tendency of the BaBar data. This, however, is at the cost of a rather small charge radius, $\langle \sqrt{r_\pi^2} \rangle < 0.4 \text{ fm}$ and a too hard elastic form factor. Hence, the question arises whether our light-front model is too simple, as other approaches seem to find a compromise between both data sets (however without presenting the corresponding values for the weak decay constant, charge radius and elastic form factor of the pion). Or is there an inherent tension in the experimental data which are incompatible?

2 Electromagnetic current and form factors

In the following, we briefly summarize the theoretical set-up [16]: kinematics, impulse approximation, and form factor definitions. Let us first remind that the matrix element of the electromagnetic current is given in the impulse approximation by the three-point function [30; 32; 36],

$$\langle p' | J_\mu^q | p \rangle = \frac{N_c}{(2\pi)^4} \int d^4k \text{Tr} [A_{\pi'}(k, p') S_q(k - p') J_\mu^q(p, p', k) S_q(k - p) A_\pi(k, p) S_{\bar{q}}(k)] + [q \leftrightarrow \bar{q}], \quad (1)$$

where $N_c = 3$ is the color number, $J_\mu^q = \bar{q} \gamma_\mu q$ is the electromagnetic current¹ and the dressed quark propagator is $S_q(p) = 1/(\not{p} - M + i\epsilon)$ with the constant quark mass M . The vertex functions, $A_{\pi, \pi'}$,

¹ since in the light-front model the quark-mass function is constant, $M(p^2) = M(p'^2) = M$, and the wave function renormalization is $Z(p^2) = Z(p'^2) \simeq 1$, the Ball-Chiu ansatz [40; 41] for the dressed quark-photon vertex reduces to the bare form γ_μ . In an approach where the mass is generated dynamically, this amounts

represents the Bethe-Salpeter amplitude which projected onto the light-front hyper-surface yields the valence wave function of the pion [31; 32]. The elastic form factor is extracted from the electromagnetic current via,

$$\langle \pi(p') | J_\mu^q(q^2) | \pi(p) \rangle = (p + p')_\mu F_\pi^{\text{em}}(q^2), \quad (2)$$

where $q = p' - p$. The weak decay constant of the pion is defined as,

$$\langle 0 | A_\mu(0) | \pi(p) \rangle = i\sqrt{2}f_\pi p_\mu, \quad (3)$$

whose value is experimentally well determined as $f_\pi = 92.4$ MeV [39].

Along similar lines, we formulated the $\gamma^*\gamma \rightarrow \pi^0$ transition form factor in the light-front quark-model approach [30; 31; 32; 33; 36]. The matrix element of the neutral pion decay, $\pi^0 \rightarrow \gamma\gamma$, driven by the Abelian anomaly is given by one unique CPT -invariant Lorentz structure. If one photon is off-shell, the same matrix element describes the transition amplitude $\gamma^*\gamma \rightarrow \pi^0$,

$$\langle \gamma(p') | J_\mu^q | \pi^0(p) \rangle = e^2 \epsilon_{\mu\nu\alpha\beta} \epsilon^\nu(p') q^\alpha p'^\beta F_{\gamma\pi^0}(q^2), \quad (4)$$

where $\epsilon^\nu(p')$ is the polarization of the real photon, $p = p' + q$ and $p'^2 = 0, p^2 = m_\pi^2$. Owing to the bosonic symmetrization of the amplitude, the transition amplitude receives two contributions:

$$T_{\mu\nu}(q, p') = t_{\mu\nu}(q, p') + t_{\mu\nu}(p', q). \quad (5)$$

Evaluating the traces in spinor and flavor space [43], the tensor $t_{\mu\nu}(q, p')$ is given by,

$$t_{\mu\nu} = \frac{4}{3} \frac{M^2}{f_\pi} e^2 N_c \epsilon_{\mu\nu\alpha\beta} q^\alpha p'^\beta I(q^2), \quad (6)$$

where $I(q^2)$ is the scalar loop integral,

$$I(q^2) = \int \frac{d^4k}{(2\pi)^4} \frac{1}{((p' - k)^2 - M^2 + i\epsilon)} \frac{1}{(k^2 - M^2 + i\epsilon)((p - k)^2 - M^2 + i\epsilon)}. \quad (7)$$

In Eq. (6), the normalization is a consequence of the quark-meson coupling definition in the light-front model, which is expressed by the Lagrangian ($\hbar = c = 1$) [28; 29],

$$\mathcal{L}_{\pi q}^{\text{int}} = -i \frac{M}{f_\pi} \pi \cdot \bar{q} \gamma_5 \tau q, \quad (8)$$

where π and q are, respectively, the pion field and quark wave functions and τ denotes isospin matrices. One may think of this coupling as the leading term of the full pseudoscalar Bethe-Salpeter amplitude.

After transformation to light-front variables, \mathbf{k}_\perp , $k^+ = k^0 + k^3$ and $k^- = k^0 - k^3$, and integration over the light-front energy, k^- , the final expression for the pion-to-photon transition form factor reads,

$$F_{\gamma\pi^0}(q^2) = \frac{N_c}{6\pi^3} \frac{M^2}{f_\pi} \int \frac{dx d^2K_\perp}{(1-x)} \frac{1}{((\mathbf{K} + x\mathbf{q})_\perp^2 + M^2)(m_\pi^2 - M_0^2)}, \quad (9)$$

where m_π is the pion mass and the reference frame is chosen such that $q^+ = q^- = 0$ and the momentum transfer, q_\perp , is transversal. The free-mass operator, M_0 , is written in terms of the momentum fraction, $x = k^+/p^+$ ($0 < x < 1$), and the relative transverse $\bar{q}q$ momentum, $\mathbf{K}_\perp = (1-x)\mathbf{k}_\perp - x(\mathbf{p} - \mathbf{k})_\perp$, as:

$$M_0^2(K_\perp^2, x) = \frac{K_\perp^2 + M^2}{x(1-x)}. \quad (10)$$

Moreover, in the soft (chiral) pion limit, the transition form factor becomes [43]:

$$F_{\gamma\pi^0}(0) = \frac{1}{4\pi^2 f_\pi} \quad (11)$$

to treating the light quarks as ‘‘heavy constituent quarks’’ whose mass is constant for all values of p^2 [42]. Nevertheless, the Ward-Takahashi identity is preserved in our formalism.

Table 1 The model's length scale parameter, r_{nr} , as a function of the constituent quark mass and for $f_\pi = 92.4$ MeV. The corresponding charge radii are listed next to r_{nr} for both the neutral and charged pion.

Model	$m_{u,d}$ [GeV]	r_{nr} [fm]	$\langle r_\pi^2 \rangle^{1/2}$ [fm]	$\langle r_{\pi^0}^2 \rangle^{1/2}$ [fm]
Gaussian	0.220	0.345	0.637	0.683
	0.330	0.472	0.655	0.552
Hydrogen	0.220	0.593	0.795	0.782
	0.330	0.708	0.807	0.582
Experiment			0.672±0.008 [39]	

One can also define a charge radius as the derivative of the transition form factor:

$$r_{\pi^0}^2 = 6 \left. \frac{dF_{\gamma\pi^0}(q^2)}{dq^2} \right|_{q^2=0}. \quad (12)$$

In following Refs. [28; 30], we identify an asymptotic pion wave function in Eq. (9) and introduce the following wave-function ansatz,

$$\frac{1}{-m_\pi^2 + M_0^2} \longrightarrow \frac{\pi^{\frac{3}{2}} f_\pi}{M\sqrt{M_0 N_c}} \Phi_\pi(K^2), \quad (13)$$

to mimic the soft QCD behavior at low momentum transfer and hard perturbative effects for large q^2 . The normalization of the pion wave function is:

$$\int d^3K \Phi_\pi^2(K^2) = 1. \quad (14)$$

Eventually, we arrive at the following expression for the $\gamma \rightarrow \pi^0$ form factor on the light front:

$$F_{\gamma\pi^0}(q^2) = \frac{\sqrt{N_c} M}{6\pi^{\frac{3}{2}}} \int \frac{dx d^2K_\perp}{x(1-x)\sqrt{M_0}} \frac{\Phi_\pi(K^2)}{(\mathbf{K} - x\mathbf{q})_\perp^2 + M^2}. \quad (15)$$

In the asymptotic limit, $Q^2 = -q^2 \rightarrow \infty$, pQCD predicts that $Q^2 F_{\gamma\pi^0} = 2f_\pi$ [5; 6], which we reproduce numerically with Eq. (15).

3 Results and conclusive remarks

Two models of the pion bound-state wave function in Eq. (15) are considered: a Gaussian and hydrogen-atom model [16], which both depend on a scale parameter r_{nr} . Including the constituent quark mass, M , we thus have two parameters. For the quark mass we employ common values in the light-front model of Ref. [30; 31; 32; 33; 36], whereas r_{nr} is fixed by fitting the weak decay constant [30; 39]: The explicit expressions are written as,

$$\begin{aligned} \Phi_\pi(K^2(\mathbf{K}_\perp; x)) &= \mathcal{N}_\pi \exp\left[-\frac{4}{3} r_{\text{nr}}^2 K^2\right], \\ \Phi_\pi(K^2(\mathbf{K}_\perp; x)) &= \frac{\mathcal{N}_\pi}{[r_{\text{nr}}^2 + K^2]^2}, \end{aligned} \quad (16)$$

with $K^2(\mathbf{K}_\perp; x) = M_0^2/4 - M^2$ and where \mathcal{N}_π is the normalization of the wave function.

In Table 1, we list a range of model parameters which describe reasonable well the charge radius of the pion and reproduce exactly the experimental value for the weak decay constant. The corresponding $F_{\gamma\pi}(q^2)$ form factor are plotted for the two models and masses in the left panel of Figure 1. As can be seen, with a constituent-mass value $M = 330$ MeV, the form factor considerably underestimates the experimental data. This is consistent with application of the model to the elastic form factor for

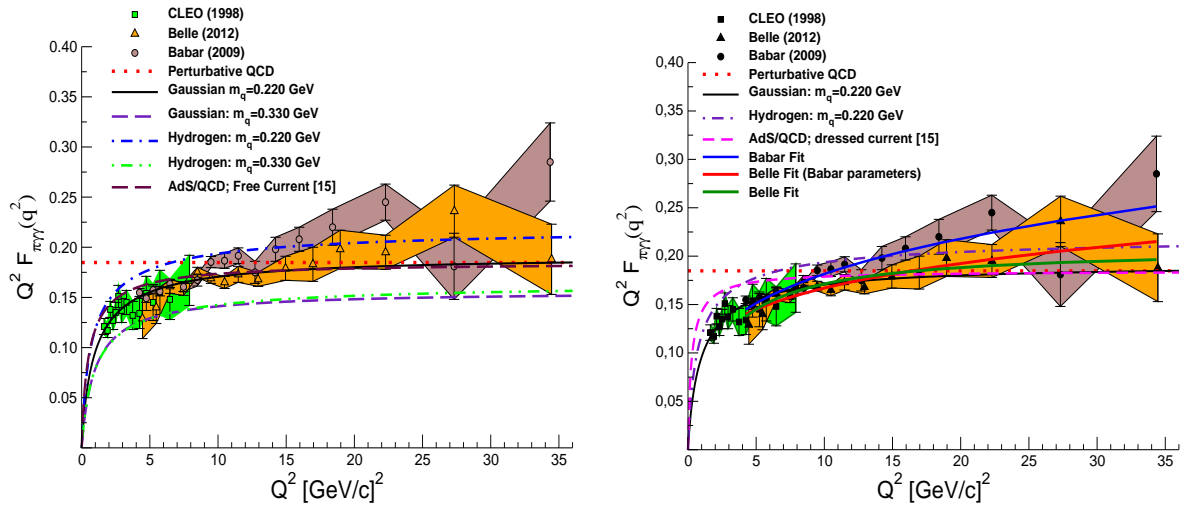


Fig. 1 The momentum weighted $F_{\gamma\pi}$ transition form factor. In the left panel we compare the light-front model for two sets of wave functions and masses with experimental data [1; 3; 4] and the AdS/QCD model expression in Eq. (17). In the right panel, the light-front wave-function model which describes most successfully *all* pion observables is plotted along with the AdS/QCD-model transition form factor in Eq. (18) and the BaBar and Belle fits (see text below).

which $M = 220$ MeV also provides the best description of the data. Moreover, while the hydrogen model accommodates the BaBar data above 10 GeV^2 , its hardness below this value is incompatible with both the BaBar, Belle and earlier CLEO data. As discussed in Ref. [16], the Gaussian model with the parameters $M = 220$ MeV and $r_{\text{nr}} = 0.345$ fm provides overall the most satisfying description of the pion's static observables and form factors; in Figure 1 this wave function corresponds to the solid (black) curve.

For comparison, we plot in the right panel of Figure 1 the transition form factor for both models and $M = 220$ MeV along with empirical fits, for which we use BaBar's parametric expression for their data [1], its application to the Belle data [4], as well as Belle's own parametrization of their data. They follow below in this order:

$$\begin{aligned} \text{BaBar: } Q^2|F(Q^2)| &= A \left(\frac{Q^2}{10 \text{ GeV}^2}\right)^\beta \implies \begin{cases} A = 0.182 \pm 0.002 \text{ GeV} \\ \beta = 0.250 \pm 0.02 \text{ GeV} \end{cases} \\ \text{Belle: } Q^2|F(Q^2)| &= A_1 \left(\frac{Q^2}{10 \text{ GeV}^2}\right)^{\beta_1} \implies \begin{cases} A_1 = 0.167 \pm 0.0036 \text{ GeV} \\ \beta_1 = 0.204 \pm 0.033 \end{cases} \\ \text{Belle: } Q^2|F(Q^2)| &= \frac{B Q^2}{Q^2 + C} \implies \begin{cases} B = 0.209 \pm 0.016 \text{ GeV} \\ C = 2.2 \pm 0.8 \text{ GeV}^2 \end{cases} \end{aligned}$$

As mentioned before, for momentum-squared values above above 10 GeV^2 , the hydrogen model is most apt at providing a reasonable description of the BaBar measurement. The functional form of $F_{\gamma\pi}(q^2)$ obtained in this domain (e.g., the dash-dotted indigo curve in the right panel of Figure 1) is compatible above $Q^2 > 10 \text{ GeV}^2$ with the application of the BaBar parametrization to both data sets, namely the blue and red solid lines.

In Figure 1, we also compare our light-front model with an application of light-front holography following Brodsky *et al.* [15], which is based on the AdS/CFT duality. The transition form factor computed in light-front holography is given by,

$$Q^2 F_{\gamma\pi^0}(Q^2) = \frac{4}{\sqrt{3}} \int_0^1 dx \frac{\phi_\pi(x)}{1-x} \left[1 - \exp\left(-\frac{(1-x)P_{q\bar{q}}Q^2}{4\pi^2 f_\pi^2 x}\right) \right], \quad (17)$$

where $\phi(x) = \sqrt{3}f_\pi x(1-x)$ is the asymptotic pion distribution function and $P_{q\bar{q}}$ is the probability to find the valence $q\bar{q}$ state. The value $P_{q\bar{q}} = 1$ is consistent with the leading-order pQCD result [6]. In case of a dressed current (see Eq. (35) in Ref. [15]), which effectively corresponds to a superposition

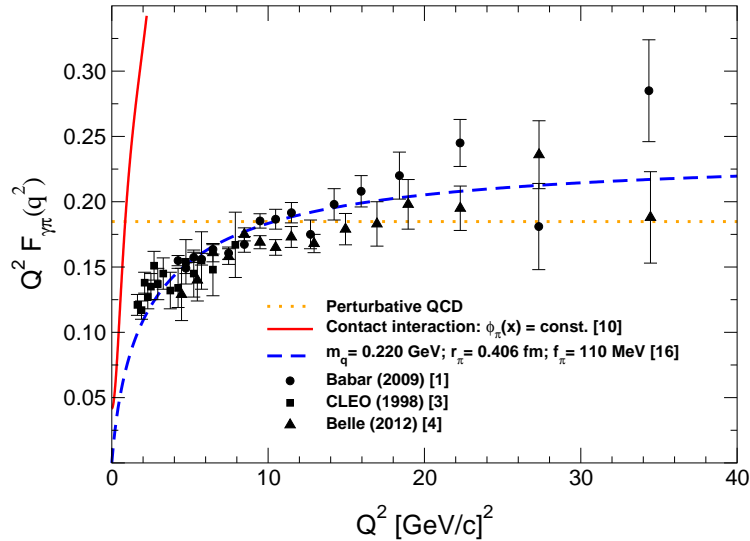


Fig. 2 The effect of a decreasing pion charge radius is demonstrated with the blue dashed curve: the Gaussian wave function ansatz in the present light-front model is adjusted so that the functional form of $F_{\gamma\pi}(Q^2)$ is in mutual agreement with the BaBar and Belle data sets for $Q^2 > 10 \text{ GeV}^2$ and likewise reproduces the data for lower four-momentum transfer. As a consequence, the charge radius decreases considerably while the weak decay constant increases. Taken to an extreme, a self-consistently regularized and symmetry-preserving contact interaction model [10] describes the pion as a point-like particle with, $\phi_\pi(x) = C \forall x \in [0, 1]$, and yields the transition form factor plotted as a red solid curve.

of Fock states, and using a twist-2 distribution function for $\Phi_\pi(x)$, the form factor is modified to,

$$Q^2 F_{\gamma\pi^0}(Q^2) = 8f_\pi \int_0^1 dx \frac{1-x}{(1+x)^3} \left[1 - x Q^2 P_{qq}/(8\pi^2 f_\pi^2) \right], \quad (18)$$

which is represented by the dashed magenta curve in the right panel of Figure 1.

The two form factor expressions obtained in the AdS/QCD models reproduce the asymptotic pQCD prediction [6], $Q^2 F_{\gamma\pi} = 2f_\pi$, and are in agreement with the Belle data at larger q^2 and our Gaussian wave function ansatz with $M = 220 \text{ MeV}$ (black solid curve). They are thus in contradiction with the BaBar data above, say, 20 GeV^2 .

We close this presentation with a last comparison in Figure 2. In there, we adapt the wave function parameter r_{nr} of the Gaussian wave function ansatz which best simultaneously and self-consistently reproduces the static pion and form factor data (black solid curve in Figure 1). This leads to a transition form factor which partially accounts for the rising tendency of the BaBar data, yet yields a rather small charge radius, $\langle \sqrt{r_\pi^2} \rangle \simeq 0.4 \text{ fm}$. Moreover, the elastic form factor using this modified wave function is too hard and in conflict with all experimental data [16]. This is qualitatively in agreement with the result obtained by means of a vector-vector contact interaction applied to the Bethe-Salpeter and gap equations in rainbow-ladder truncation. Since this interaction leads to quadratic divergences, it must be treated with a symmetry-preserving regularization [10]. The consequences of this interaction are a constant constituent-like quark mass and a point-like pion with a flat distribution amplitude, $\phi_\pi(x) = C$, which implies that all form factors asymptotically approach a constant. This behavior is observed in the red solid curve in Figure 2 which corresponds to the self-consistent rainbow-ladder treatment of the contact interaction.

Acknowledgements This work was supported by the São Paulo State Research Foundation (FAPESP) under grants nos. 2009/00069-5, 2009/53351-0, 2009/51296-1 and 2012/17396-1. T. Frederico also acknowledges support by the National Council for Scientific and Technological Development (CNPq). J. P. B. C. de Melo and T. Frederico thank Nicos Stefanis for the LC2013 organization and the invitation. B. El-Bennich appreciated helpful communication with Adnan Bashir and is grateful to Laura Xiomara Gutiérrez-Guerrero for providing the transition form factor data in Figure 2.

References

1. B. Aubert *et al.* [BaBar Collaboration], Phys. Rev. D **80**, 052002 (2009).
2. H. J. Behrend *et al.* [CELLO Collaboration], Z. Phys. C **49**, 401 (1991).
3. J. Gronberg *et al.* [CLEO Collaboration], Phys. Rev. D **57**, 33 (1998).
4. S. Uehara *et al.* [Belle Collaboration], Phys. Rev. D **86**, 092007 (2012).
5. G. R. Farrar and D. R. Jackson, Phys. Rev. Lett. **43**, 246 (1979).
6. G. P. Lepage and S. J. Brodsky, Phys. Rev. D **22** (1980) 2157.
7. J. Segovia, L. Chang, I. C. Cloët, C. D. Roberts, S. M. Schmidt and H.-S. Zong, arXiv:1311.1390 [nucl-th].
8. I. C. Cloët, L. Chang, C. D. Roberts, S. M. Schmidt and P. C. Tandy, Phys. Rev. Lett. **111**, 092001 (2013).
9. L. Chang, I. C. Cloët, J. J. Cobos-Martínez, C. D. Roberts, S. M. Schmidt and P. C. Tandy, Phys. Rev. Lett. **110**, 132001 (2013).
10. H. L. L. Roberts, C. D. Roberts, A. Bashir, L. X. Gutiérrez-Guerrero, and P. C. Tandy, Phys. Rev. **C82**, 065202 (2010).
11. N. Stefanis, Few Body Syst. **52**, 415 (2011), 1109.2718.
12. A. Bakulev, S. Mikhailov, A. Pimikov, and N. Stefanis, Phys. Rev. **D84**, 034014 (2011).
13. A. Bakulev, S. Mikhailov, A. Pimikov, and N. Stefanis, Phys. Rev. **D86**, 031501(2012).
14. S. J. Brodsky, F.-G. Cao, and G. F. de Téra mond, Phys. Rev. **D84**, 033001 (2011).
15. S. J. Brodsky, F.-G. Cao, and G. F. de Téra mond, Phys. Rev. **D84**, 075012 (2011).
16. B. El-Bennich, J. P. B. C. de Melo and T. Frederico, Few Body Syst. **54**, 1851 (2013).
17. D. G. Dumm, S. Noguera, N. N. Scoccola and S. Scopetta, arXiv:1311.3595 [hep-ph].
18. A. V. Radyushkin, Phys. Rev. **D80**, 094009 (2009).
19. A. E. Dorokhov, JETP Lett. **92**, 707 (2010).
20. P. Kroll, Eur. Phys. J. **C71**, 1623 (2011),.
21. X.-G. Wu and T. Huang, Phys. Rev. **D82**, 034024 (2010).
22. S. S. Agaev, V. M. Braun, N. Offen, and F. A. Porkert,
23. P. Maris and C. D. Roberts, Phys. Rev. C **56**, 3369 (1997).
24. S. Aoki *et al.* [PACS-CS Collaboration], Phys. Rev. D **79**, 034503 (2009).
25. W. Bietenholz, M. Gockeler, R. Horsley, Y. Nakamura, D. Pleiter, P. E. L. Rakow, G. Schierholz and J. M. Zanotti, Phys. Lett. B **687**, 410 (2010).
26. A. Bashir, L. Chang, I. C. Cloet, B. El-Bennich, Y.-X. Liu, C. D. Roberts and P. C. Tandy, Commun. Theor. Phys. **58**, 79 (2012).
27. I. C. Cloët and C. D. Roberts, arXiv:1310.2651 [nucl-th].
28. T. Frederico and G. A. Miller, Phys. Rev. D **45**, 4207 (1992).
29. T. Frederico and G. A. Miller, Phys. Rev. D **50**, 210 (1994).
30. J. P. C. B. de Melo, H. W. L. Naus and T. Frederico, Phys. Rev. C **59**, 2278 (1999).
31. J. P. B. C. de Melo, T. Frederico, E. Pace and G. Salmè, Nucl. Phys. A **707**, 399 (2002).
32. J. P. B. C. de Melo, T. Frederico, E. Pace and G. Salmè, Phys. Lett. B **581**, 75 (2004).
33. J. P. B. C. de Melo, T. Frederico, E. Pace, and G. Salmè, Phys. Rev. D **73**, 074013 (2006).
34. B. L. G. Bakker, A. Bassetto, S. J. Brodsky, W. Broniowski, S. Dalley, T. Frederico, S. D. Glazek and J. R. Hiller *et al.*, arXiv:1309.6333 [hep-ph].
35. S. J. Brodsky, G. F. de Tramond and H. G. Dosch, arXiv:1310.8648 [hep-ph].
36. B. El-Bennich, J. P. B. C. de Melo, B. Loiseau, J.-P. Dedonder and T. Frederico, Braz. J. Phys. **38**, 465 (2008).
37. C. S. Mello, J. P. C. Filho, E. O. da Silva, B. El-Bennich, J. P. B. C. de Melo and V. S. Filho, AIP Conf. Proc. **1520**, 333 (2013).
38. E. O. da Silva, J. P. B. C. de Melo, B. El-Bennich and V. S. Filho, Phys. Rev. C **86**, 038202 (2012).
39. J. Beringer *et al.* [Particle Data Group Collaboration], Phys. Rev. D **86**, 010001 (2012).
40. J. S. Ball and T.-W. Chiu, Phys. Rev. D **22**, 2542 (1980); *ibid.* D **22**, 2550 (1981).
41. E. Rojas, J. P. B. C. de Melo, B. El-Bennich, O. Oliveira and T. Frederico, JHEP **1310**, 193 (2013).
42. B. El-Bennich, M. A. Ivanov and C. D. Roberts, Nucl. Phys. Proc. Suppl. **199**, 184 (2010).
43. C. Itzykson and J.-B. Zuber, *Quantum Field Theory*, International Series In Pure and Applied Physics (McGraw-Hill, New York, 1980).